

IEM-FT-114/95
hep-ph/9509385**STATUS OF EFFECTIVE POTENTIAL CALCULATIONS** *

M. Quirós †

*CERN, TH Division, CH-1211 Geneva 23, Switzerland***Abstract**

We review various effective potential methods which have been useful to compute the Higgs mass spectrum and couplings of the minimal supersymmetric standard model. We compare results where all-loop next-to-leading-log corrections are resummed by the renormalization group, with those where just the leading-log corrections are kept. Pole masses are obtained from running masses by addition of convenient self-energy diagrams. Approximate analytical expressions are worked out, providing an excellent approximation to the numerical results which include all next-to-leading-log terms. An appropriate treatment of squark decoupling allows to consider large values of the stop and/or sbottom mixing parameters and thus fix a reliable upper bound on the mass of the lightest CP-even Higgs boson mass.

IEM-FT-114/95
September 1995

*Based on talk given at the *SUSY-95 International Workshop on Supersymmetry and Unification of Fundamental Interactions*, Palaiseau, 15-19 May 1995.

†On leave of absence from Instituto de Estructura de la Materia, CSIC, Serrano 123, 28006-Madrid, Spain. Work supported in part by the European Union (contract CHRX-CT92-0004) and CICYT of Spain (contract AEN94-0928).

1 Introduction

The **effective potential** methods to compute the (radiatively corrected) Higgs mass spectrum in the Minimal Supersymmetric Standard Model (MSSM) are useful since they allow to **resum** (using Renormalization Group (RG) techniques) leading-log (LL), next-to-leading-log (NTLL),..., corrections to **all orders** in perturbation theory. These methods [1, 2], as well as the diagrammatic methods [3] to compute the Higgs mass spectrum in the MSSM, were first developed in the early nineties.

Effective potential methods are based on the **run-and-match** procedure by which all dimensionful and dimensionless couplings are running with the RG scale, for scales greater than the masses involved in the theory. When the RG scale equals a particular mass threshold, heavy fields decouple, eventually leaving threshold effects in order to match the effective theory below and above the mass threshold. For instance, assuming a common soft supersymmetry breaking mass for left-handed and right-handed stops and sbottoms, $M_S \sim m_Q \sim m_U \sim m_D$, and assuming for the top-quark mass, m_t , and for the CP-odd Higgs mass, m_A , the range $m_t \leq m_A \leq M_S$, we have: for scales $Q \geq M_S$, the MSSM, for $m_A \leq Q \leq M_S$ the two-Higgs doublet model (2HDM), and for $m_t \leq Q \leq m_A$ the Standard Model (SM). Of course there are thresholds effects at $Q = M_S$ to match the MSSM with the 2HDM, and at $Q = m_A$ to match the 2HDM with the SM.

The neutral Higgs sector of the MSSM contains, on top of the CP-odd Higgs A , two CP-even Higgs mass eigenstates, H_h (the heaviest one) and H (the lightest one). It turns out that the larger m_A the heavier the lightest Higgs H . Therefore the case $m_A \sim M_S$ is, not only a great simplification since the effective theory below M_S is the SM, but also of great interest, since it provides the upper bound on the mass of the lightest Higgs (which is interesting for phenomenological purposes, e.g. at LEP 2). In this case the threshold correction at M_S for the SM quartic coupling λ is:

$$\Delta_{\text{th}}\lambda = \frac{3}{16\pi^2} h_t^4 \frac{X_t^2}{M_S^2} \left(2 - \frac{1}{6} \frac{X_t^2}{M_S^2} \right) \quad (1)$$

where h_t is the SM top Yukawa coupling and $X_t = (A_t - \mu / \tan \beta)$ is the mixing in the stop mass matrix, the parameters A_t and μ being the trilinear soft-breaking coupling in the stop sector and the supersymmetric Higgs mixing mass, respectively. The maximum of (1) corresponds to $X_t^2 = 6M_S^2$ which provides the maximum value of the lightest Higgs mass: this case will be referred to as the case of maximal mixing.

2 Leading-log vs Next-to-leading-log results

Recent effective potential studies [4] have proved that the L-loop improved effective potential, with (L+1)-loop RG equations is exact to Lth-to-leading-log order. In particular the case L=0 (tree level potential improved with one-loop RG) describes the LL approximation, and the case L=1 (one-loop effective potential improved with two-loop RG) describes the NTLL approximation. In particular, the effective potential in the NTLL approximation is expected to be highly scale independent. But, can we quantify the scale independence of it?

We have minimized the effective potential at the scale t^* such that [5]

$$\left. \frac{d}{dt} \frac{\Phi_{\min}(t)}{\xi(t)} \right|_{t=t^*} = 0 \quad (2)$$

where $\xi(t)$ is the anomalous dimension of the Higgs field. In fact the scale dependence is

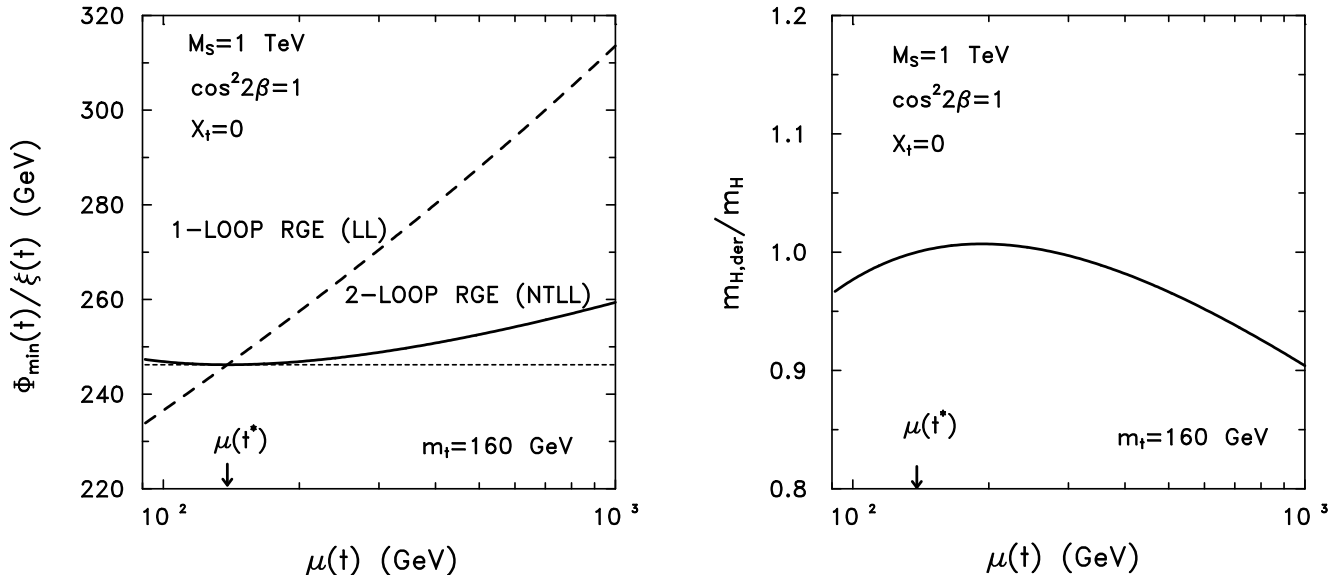


Figure 1: **Left panel:** Plot of $\phi_{\min}(t)/\xi(t)$ as a function of $\mu(t)$ in the LL (dashed line) and NTLL (solid line) approximation. The dotted line shows the would-be scale independent result. **Right panel:** Plot of $m_{H,der}(t)/m_H(t)$ as a function of $\mu(t)$. In both cases $m_t = 160$ GeV and the supersymmetric parameters are $M_S = 1$ TeV, $X_t = 0$ and $\tan \beta \gg 1$.

measured by the quantity $\Phi_{\min}(t)/\xi(t)$, which is constant for a scale invariant theory. We have plotted it versus the RG scale $\mu(t)$ in Fig. 1 (left panel) where we can see that the best minimization scale $\mu(t^*)$ is around the value of the running top-quark mass and that minimizing the effective potential at the high scale M_S produces a departure of the scale invariance of $\Phi_{\min}(t)/\xi(t)$ of order 10%. This measure of scale invariance is associated with the minimum of the potential, i.e. with the first derivative. An independent measure, associated with the second derivative of the effective potential, is given by the ratio $m_{H,der}/m_H$, where $m_{H,der}$ is the second derivative of the potential at the scale $\mu(t)$ and m_H the second derivative at the minimization scale $\mu(t^*)$, run to the scale $\mu(t)$ with the anomalous dimension of the Higgs field. The corresponding plot is shown in Fig. 1 (right panel) where we can see a similar tendency in the sense that the ratio $(m_{H,der} - m_H)/m_H$ is $\mathcal{O}(10)\%$ for large values of the scale $\mu(t)$. This feature of $\mu(t^*)$ being close to the top-quark running mass on shell (i.e. $m_t(Q = m_t) = m_t$) remains for all values of the top-quark mass and supersymmetric parameters, as in Fig. 2.

We also have defined physical (pole) masses for the top quark and the Higgs boson. For the top-quark we have included the usual one-loop QCD corrections, and for the Higgs boson one-loop electroweak corrections as

$$M_H^2 = m_H^2(t) + \text{Re} \left[\Pi_{HH}(M_H^2) - \Pi_{HH}(0) \right] \quad (3)$$

where $m_H(t)$ is the running Higgs mass and Π_{HH} the Higgs self-energies which can be found in Ref. [5]. We have plotted in Fig. 3 M_H as a function of $\tan \beta$ (left panel) and as a function of M_t (right panel). From Fig. 3 we can see that the present experimental band from CDF/D0

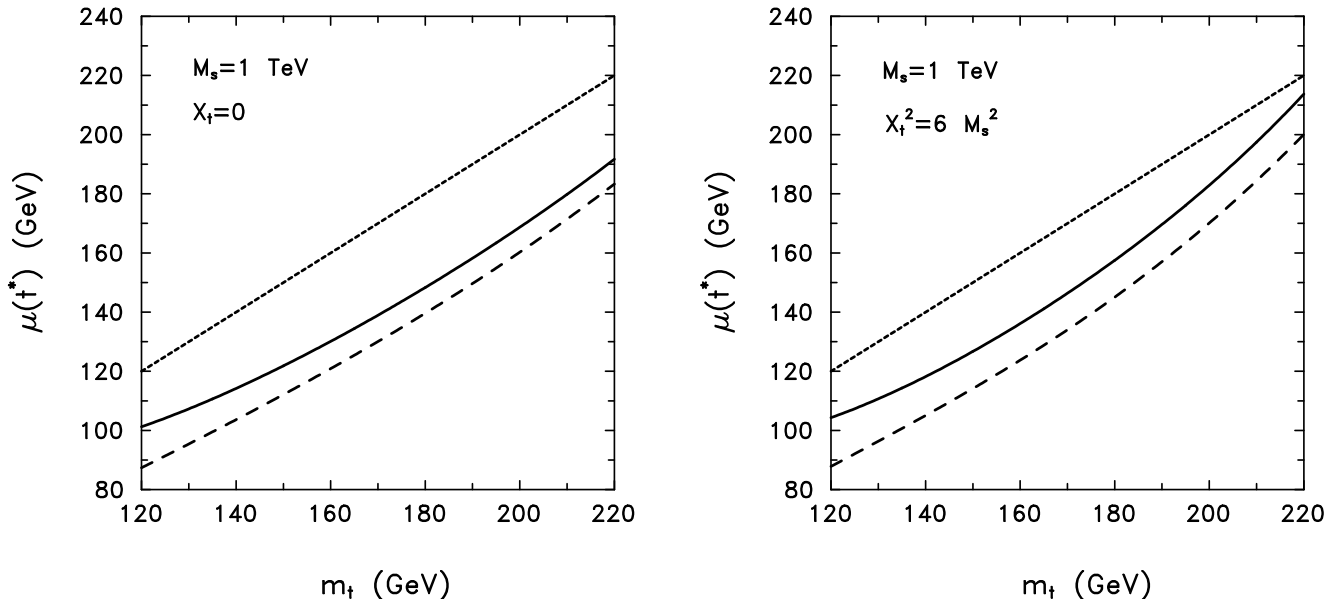


Figure 2: Plot of $\mu(t)^*$ as a function of m_t for $\tan\beta \gg 1$ (solid lines), $\tan\beta = 1$ (dashed lines), and supersymmetric parameters $M_S = 1$ TeV, $X_t = 0$ (left panel) and $X_t^2 = 6M_S^2$ (right panel). The dotted lines correspond to $\mu(t^*) = m_t$.

for the top-quark mass requires $M_H \lesssim 140$ GeV, while if we fix $M_t = 170$ GeV, then the upper bound $M_H \lesssim 125$ GeV follows. It goes without saying that these figures are extremely relevant for MSSM Higgs searches at LEP 2.

3 Comparison with other approaches

It is worth at this point to compare our NTLL calculation with other similar calculations aiming to evaluate two-loop corrections to the lightest Higgs mass in the MSSM. For this purpose we have plotted in Fig. 4 M_H as a function of the minimization scale $\mu(t^*)$ for different values of supersymmetric parameters, and for the LL (dashed lines) and NTLL (solid lines) approximations. We can see that our definition of pole mass (3) provides a highly scale independent Higgs mass in the NTLL approximation. Moreover, as was the case in Fig. 1 (left panel), the LL approximation exhibits a strong dependence with the minimization scale.

□ Kodaira, Yasui and Sasaki [6] have used an effective potential method neglecting gauge couplings in the one-loop correction to the effective potential ($g = g' = 0$) and neglecting the contribution of the stop mixing to the threshold corrections ($X_t = 0$). Furthermore they have not introduced any wave function renormalization for the Higgs and thus have worked with running Higgs masses. Finally they have chosen as minimization scale $\mu(t^*) = v = 246.22$ GeV and claimed that the difference between the NTLL and the LL approximations is positive and sizeable, unlike a previous result in Ref. [2] where it was claimed it to be negative and small. A quick glance at Fig. 4 allows to understand these seemingly contradictory results. We have plotted with a □ the minimization scale chosen in Ref. [6] and with a ◇ our choice. Had we chosen as minimization scale the □ we had found (even if our analysis includes gauge

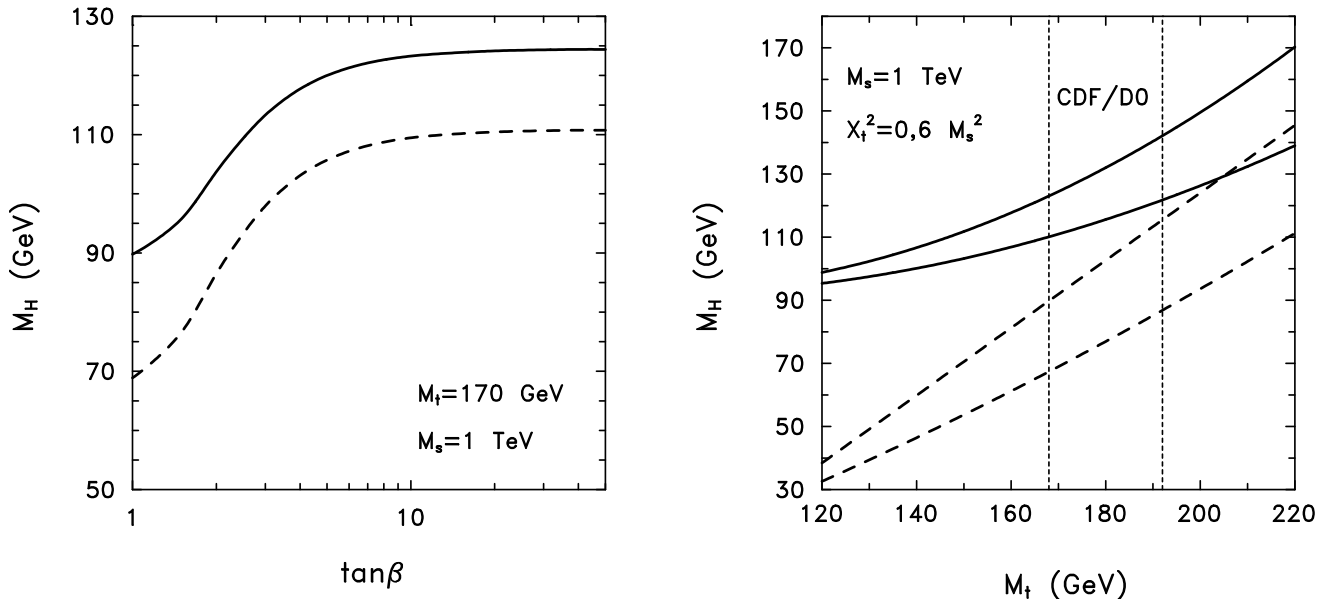


Figure 3: **Left panel:** Plot of M_H as a function of $\tan\beta$ for $M_t = 170$ GeV and $M_s = 1$ TeV. The solid (dashed) curve corresponds to the $X_t^2 = 6M_s^2$ ($X_t = 0$) case. **Right panel:** Plot of M_H as a function of M_t for $\tan\beta \gg 1$ (solid lines), $\tan\beta = 1$ (dashed lines), and $X_t^2 = 6M_s^2$ (upper set), $X_t = 0$ (lower set). The experimental band from the CDF/D0 detection is also indicated.

coupling effects and considers pole masses) that (NTLL–LL) is positive and sizeable. However our choice of the minimization scale at the \diamond position suggests (NTLL–LL) negative and tiny. Since we made our choice of the minimization scale such that the effective potential is as scale independent as possible we could say that the latter statement is the correct one. However, since we have defined pole (scale independent) masses for the Higgs boson (unlike in Ref. [6]) in the NTLL approximation, and the LL approximation is strongly scale dependent, the quantity (NTLL–LL) is scale dependent and then meaningless to qualify the goodness of the approximation.

\triangle Langacker and Polonsky [7] work in the LL approximation and fix as minimization scale $\mu(t^*) = M_Z$. They find larger values than those in Fig. 3. We have plotted in Fig. 4 their minimization scale with a \triangle . We can easily see that for that scale the two-loop corrections that they disregard are large and negative. Had they evaluated them they should have found similar results to ours.

\diamond Finally, Hempfling and Hoang [8] use diagrammatic and effective potential approaches to evaluate the lightest Higgs mass at two-loop order. They use various approximations, as e.g. $g = g' = 0$ in the effective potential and only deal with the case of zero stop mixing, $X_t = 0$. Their results contain LL and NTLL corrections to one- and two-loop orders, while our LL and NTLL corrections are resummed to all-loop by the RG. However, in the case of no mixing, where we can compare both approaches, our results agree within ~ 2 -3 GeV, which we consider as fully satisfactory, given all their simplifications and the fact that this corresponds to the uncertainty of our own calculation, due to the tiny scale dependence of the effective potential and pole masses, and other small effects as, e.g., the possible presence of light charginos and

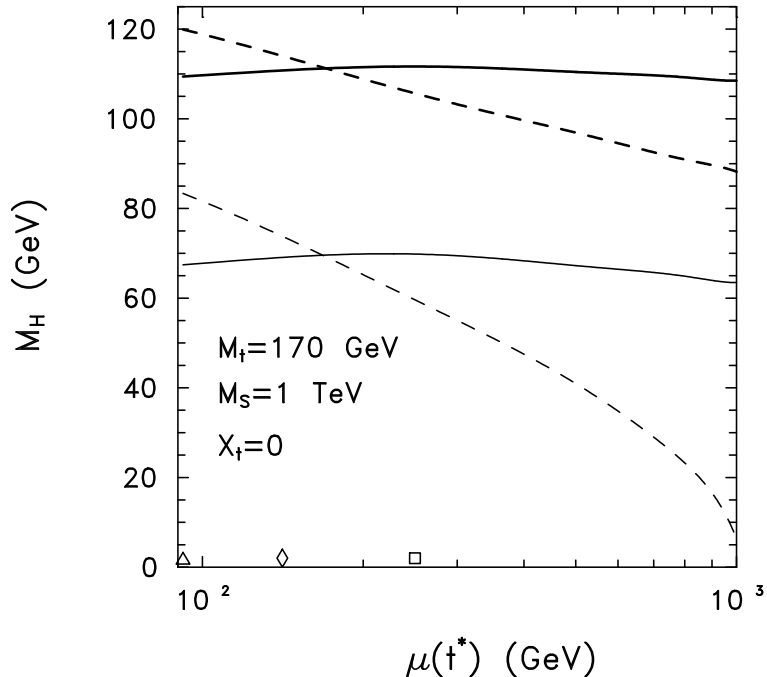


Figure 4: Plot of M_H as a function of $\mu(t^*)$ for $M_t = 170$ GeV, $M_S = 1$ TeV and $X_t = 0$. The solid (dashed) curves correspond to the NTLL (LL) approximation, and the upper (lower) set to $\tan\beta \gg 1$ ($\tan\beta = 1$).

neutralinos.

4 An analytical approximation

We have seen from Figs. 1 and 2, and previous considerations that, since radiative corrections are minimized for scales $Q \sim m_t$, when the LL RG improved Higgs mass expressions [9] are evaluated at the top-quark mass scale, they reproduce the NTLL value with a high level of accuracy, for any value of $\tan\beta$ and the stop mixing parameters [10]

$$m_{H,LL}(Q^2 \sim m_t^2) \sim m_{H,NTLL}. \quad (4)$$

Based on the above observation, we can work out a very accurate analytical approximation to $m_{H,NTLL}$ by just keeping two-loop LL corrections at $Q^2 = m_t^2$, i.e. corrections of order t^2 , where $t = \log(M_S^2/m_t^2)$.

Again the case $m_A \sim M_S$ is the simplest, and very illustrative, one. We have found [10, 11] that, in the absence of mixing (the case $X_t = 0$) two-loop corrections resum in the one-loop result shifting the energy scale from M_S (the tree-level scale) to $\sqrt{M_S m_t}$. More explicitly,

$$m_H^2 = M_Z^2 \cos^2 2\beta \left(1 - \frac{3}{8\pi^2} h_t^2 t \right) + \frac{3}{2\pi^2 v^2} m_t^4 (\sqrt{M_S m_t}) t \quad (5)$$

where $v = 246.22$ GeV.

In the presence of mixing ($X_t \neq 0$), the run-and-match procedure yields an extra piece in the SM effective potential $\Delta V_{\text{th}}[\phi(M_S)]$ whose second derivative gives an extra contribution to the Higgs mass, as

$$\Delta_{\text{th}} m_H^2 = \frac{\partial^2}{\partial \phi^2(t)} \Delta V_{\text{th}}[\phi(M_S)] = \frac{1}{\xi^2(t)} \frac{\partial^2}{\partial \phi^2(t)} \Delta V_{\text{th}}[\phi(M_S)] \quad (6)$$

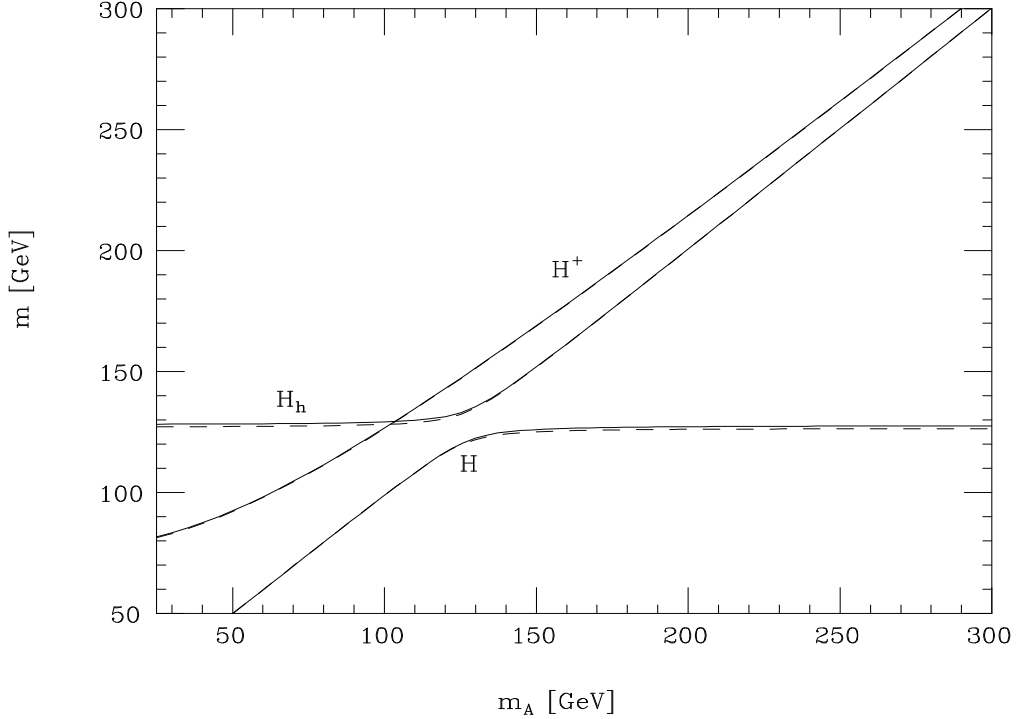


Figure 5: The neutral (H_h, H) and charged (H^+) Higgs mass spectrum as a function of the CP-odd Higgs mass m_A for a physical top-quark mass $M_t = 175$ GeV and $M_S = 1$ TeV, as obtained from the one-loop improved RG evolution (solid lines) and the analytical formulae (dashed lines). All sets of curves correspond to $\tan\beta = 15$ and large squark mixing, $X_t^2 = 6M_S^2$ ($\mu = 0$).

which, in our case, reduces to

$$\Delta_{\text{th}} m_H^2 = \frac{3}{4\pi^2} \frac{m_t^4(M_S)}{v^2(m_t)} \frac{X_t^2}{M_S^2} \left(2 - \frac{1}{6} \frac{X_t^2}{M_S^2} \right) \quad (7)$$

We have compared our analytical approximation [10] with the numerical NTLL result [5] and found a difference $\lesssim 2$ GeV for all values of supersymmetric parameters.

The case $m_A < M_S$ is a bit more complicated since the effective theory below the supersymmetric scale M_S is the 2HDM. However since radiative corrections in the 2HDM are equally dominated by the top-quark, we can compute analytical expressions based upon the LL approximation at the scale $Q^2 \sim m_t^2$. This has been done in Ref. [10] where LL are resummed to two-loop. Our approximation differs from the LL all-loop numerical resummation by $\lesssim 3$ GeV, which we consider the uncertainty inherent in the theoretical calculation, provided the mixing is moderate and, in particular, bounded by the condition,

$$\left| \frac{m_{\tilde{t}_1}^2 - m_{\tilde{t}_2}^2}{m_{\tilde{t}_1}^2 + m_{\tilde{t}_2}^2} \right| \lesssim 0.5 \quad (8)$$

where $\tilde{t}_{1,2}$ are the two stop mass eigenstates. In Fig. 5 the Higgs mass spectrum is plotted versus m_A .

5 Threshold effects

There are two possible caveats in the approximation we have just presented: **i)** Our expansion parameter $\log(M_S^2/m_t^2)$ does not behave properly in the supersymmetric limit $M_S \rightarrow 0$, where we should recover the tree-level result. **ii)** We have expanded the threshold function $\Delta V_{\text{th}}[\phi(M_S)]$ to order X_t^4 . In fact keeping the whole threshold function $\Delta V_{\text{th}}[\phi(M_S)]$ we would be able to go to larger values of X_t and to evaluate the accuracy of the approximation (1) and (7). Only then we will be able to check the reliability of the maximum value of the lightest Higgs mass (which corresponds to the maximal mixing) as provided in the previous sections. This procedure has been properly followed in Refs. [10] and [12], where the most general case

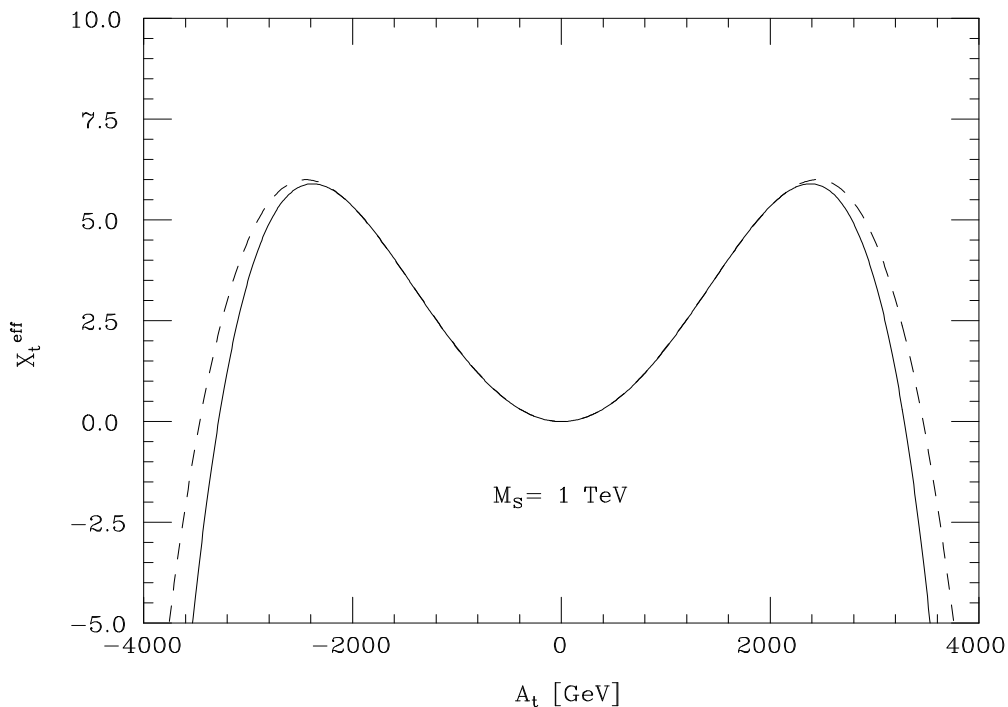


Figure 6: Plot of the exact (solid line) and approximated (dashed line) effective mixing X_t^{eff} as a function of A_t , for $M_S = 1$ TeV and $\mu = 0$.

$m_Q \neq m_U \neq m_D$ has been considered. We have proved that keeping the exact threshold function $\Delta V_{\text{th}}[\phi(M_S)]$, and properly running its value from the high scale to m_t with the corresponding anomalous dimensions as in (6), produces two effects: **i)** It makes a resummation from M_S^2 to $M_S^2 + m_t^2$ and generates as (physical) expansion parameter $\log[(M_S^2 + m_t^2)/m_t^2]$. **ii)**

It generates a whole threshold function X_t^{eff} such that (7) becomes

$$\Delta_{\text{th}} m_H^2 = \frac{3}{4\pi^2} \frac{m_t^4 [M_S^2 + m_t^2]}{v^2(m_t)} X_t^{\text{eff}} \quad (9)$$

and

$$X_t^{\text{eff}} = \frac{X_t^2}{M_S^2 + m_t^2} \left(2 - \frac{1}{6} \frac{X_t^2}{M_S^2 + m_t^2} \right) + \dots \quad (10)$$

In fact we have plotted X_t^{eff} as a function of A_t (solid line) and compared with the approximation where we keep only terms up to X_t^4 (dashed line), as we did in the previous sections. The result shows that the maximum of both curves are very close to each other, what justifies the reliability of previous upper bounds on the lightest Higgs mass as, e.g., in Fig. 3.

6 Conclusions

We have seen that effective potential methods, when decoupling is properly accounted for, are useful and powerful techniques to analyze the MSSM Higgs sector and provide easy-to-use analytical approximations (with radiative corrections RG resummed) to the Higgs mass spectrum and couplings. In particular, an appropriate treatment of stop and sbottom decoupling allows to consider large mixing parameters and put reliable upper bounds on the lightest Higgs boson mass in the MSSM.

References

- [1] Y. Okada, M. Yamaguchi and T. Yanagida, *Prog. Theor. Phys.* **85** (1991) 1; *Phys. Lett.* **B262** (1991) 54; J. Ellis, G. Ridolfi and F. Zwirner, *Phys. Lett.* **B257** (1991) 83; *Phys. Lett.* **B262** (1991) 477; R. Barbieri and M. Frigeni, *Phys. Lett.* **B258** (1991) 395; R. Barbieri, M. Frigeni and F. Caravaglios, *Phys. Lett.* **B258** (1991) 167
- [2] J.R. Espinosa and M. Quirós, *Phys. Lett.* **B266** (1991) 389
- [3] H.E. Haber and R. Hempfling, *Phys. Rev. Lett.* **66** (1991) 1815; A. Yamada, *Phys. Lett.* **B263** (1991) 233
- [4] B. Kastening, *Phys. Lett.* **B283** (1992) 287; C. Ford, D.R.T. Jones, P.W. Stephenson and M.B. Einhorn, *Nucl. Phys.* **B395** (1993) 17; M. Bando, T. Kugo, N. Maekawa and H. Nakano, *Phys. Lett.* **B301** (1993) 83; *Prog. Theor. Phys.* **90** (1993) 405; C. Ford, *Phys. Rev.* **D50** (1994) 7531
- [5] J.A. Casas, J.R. Espinosa, M. Quirós and A. Riotto, *Nucl. Phys.* **B436** (1995) 3; (E) **B439** (1995) 466
- [6] J. Kodaira, Y. Yasui and K. Kasaki, *Phys. Rev.* **D50** (1994) 7035
- [7] P. Langacker and N. Polonsky, *Phys. Rev.* **D50** (1994) 2199
- [8] R. Hempfling and A.H. Hoang, *Phys. Lett.* **B331** (1994) 99

- [9] M. Carena, K. Sasaki and C.E.M. Wagner, *Nucl. Phys.* **B381** (1992) 66; H.E. Haber and R. Hempfling, *Phys. Rev.* **D48** (1993) 4280
- [10] M. Carena, J.R. Espinosa, M. Quirós and C.E.M. Wagner, *Phys. Lett.* **B355** (1995) 209
- [11] H.E. Haber, R. Hempfling and A.H. Hoang, CERN preprint, in preparation
- [12] M. Carena, M. Quirós and C.E.M. Wagner, preprint CERN-TH/95-157